

DETERMINATION OF ROCK DAMAGE CHARACTERISTICS AFTER LASER IRRADIATION BASED ON COMPUTED TOMOGRAPHY SCANNING AND THE NUCLEAR MAGNETIC RESONANCE TECHNIQUE

by

**Xue-Min ZHOU^a, Ming-Zhong GAO^{a,b*}, Jun-Jun LIU^b, Lei YANG^b,
Hai-Chun HAO^a, Tian-Xiang AO^a, Yi-Kun YANG^a, and Zhi-Qiang HE^b**

^a Guangdong Provincial Key Laboratory of Deep Earth Sciences and Geothermal Energy Exploitation and Utilization, Institute of Deep Earth Sciences and Green Energy,

College of Civil and Transportation Engineering, Shenzhen University, Shenzhen, China

^b College of Water Resource and Hydro power State, State Key Laboratory of Intelligent Construction and Healthy Operation and Maintenance of Deep Underground Engineering, Sichuan University, Chengdu, China

Original scientific paper

<https://doi.org/10.2298/TSCI2404559Z>

Efficiently crushing deep hard rock remains a significant engineering challenge. As an innovative rock-breaking technique, laser technology shows considerable promise for applications in deep engineering. Analyzing the damage characteristics of rock after laser irradiation and clarifying the mechanism of laser rock-breaking are crucial for advancing this technology towards practical engineering applications. Taking basalt as a typical representative of deep hard rock, we introduced computed tomography (CT) scanning and nuclear magnetic resonance (NMR) technology to study the internal macro and micro pore characteristics of the rock after laser irradiation with different power. Additionally, we reconstructed the morphology of the laser-drilled holes. The results show that the surface temperature of the rock under laser irradiation generally follows a Gaussian distribution, and the penetration depth of the 1250 W laser can reach 41.51 mm after 30 seconds. Laser irradiation affects the microscopic pores of the rock, causing small pores to expand into larger ones as the laser power increases. After laser irradiation, the molten holes can be categorized into drum-shaped and V-shaped zones, and the timely discharge of molten material enhances the efficiency of laser rock-breaking. These findings provide theoretical and technical support for the application of laser rock-breaking technology in the efficient crushing of deep hard rock and resource extraction.

Key words: laser irradiation, temperature distribution, CT scanning, NMR

Introduction

With the rapid development of underground resources and space, efficiently crushing deep hard rock has become a technical challenge in underground construction [1]. The *three highs and one disturbance* environment faced by deep rock makes construction more difficult. Traditional mechanical drilling often encounters problems such as low drilling speed and severe tool wear, which greatly affects construction progress [2]. Faced with the challenges posed

* Corresponding author, e-mail: gaomingzhong@163.com

by deep hard rock layers, new rock-breaking methods have emerged rapidly. Techniques such as laser [3], microwave, water jet [4], and electric pulse [5] rock-breaking have seen significant development. Among these, laser rock-breaking is a well-established method for the directional crushing of deep hard rock.

At present, many scholars have carried out exploratory research work in the field of laser rock-breaking. This method primarily uses high energy laser beams to irradiate the rock surface, generating localized high temperatures that cause the rock to melt, fracture, and evaporate [6, 7]. Yang *et al.* [8] studied the temperature distribution characteristics of basalt, sandstone and granite under laser irradiation. The results showed that the laser power and rock composition are the key factors affecting the temperature distribution, and that rock phase changes are the main reason for the uneven temperature increase. Laser thermal action can induce thermal softening of the rock, reducing its strength and drillability [9, 10]. Chen *et al.* [11] investigated the differences between circular and elliptical laser irradiation on sandstone. They proposed an elliptical laser-assisted drilling method to fracture the rock, which increased the rate of penetration (ROP) by 61% compared to conventional drilling bits. Pan *et al.* [12] investigated the effect of laser parameters on the thermal crushing characteristics of shale and monitored strain characteristics during laser irradiation. They found that strain values decrease abruptly as the rock breaks, with larger decreases occurring at the cracks.

However, most scholars currently focus on studying the temperature field, surface morphology, and macroscopic mechanical behavior, while there is relatively little research on the internal pore-forming morphology and pore structure of rocks after laser irradiation. Therefore, the introduction of CT scanning and NMR technology to analyze the macroscopic pore formation and microscopic pore before and after laser irradiation is of great significance for the practical engineering application and numerical simulation of laser rock-breaking.

Sample preparation and experimental scheme

Sample preparation and equipment

The basalt samples used in this paper were taken from Zuoquan, Shanxi, with uniform texture and gray color. They were processed into standard cylindrical samples measuring $\text{Ø}50 \text{ mm} \times 100 \text{ mm}$. The average density of the rock samples at room temperature was 2.787 g/cm^3 , and the average longitudinal wave velocity of the rock samples was 5224.48 m/s . The laser hard rock fracturing and weakening test is completed by the laser precision rock-breaking system independently developed by the group. In addition, the in-situ real-time true triaxial X-ray industrial CT inspection system was used to analyze the internal slice images and microscopic rupture morphology of the rock before and after irradiation, and the 3-D reconstruction of the internal molten hole formation of the basalt was realized by Avizo software. The changes in rock pore distribution before and after laser irradiation were analyzed using the NMR test, conducted with an LMR-30 low field NMR analyzer. The experimental equipment and set-up are illustrated in fig. 1.

Experiment scheme

The effect of laser irradiation on rock thermal cracking is affected by many factors, including laser power, irradiation time, and rock saturation state. Based on the previous study [13], the laser power has a greater influence on the thermal effect of basalt, so further research is carried out. The experiment was carried out using the controlled single-variable method, setting the laser power as 250 W, 500 W, 750 W, 1000 W, and 1250 W, the laser irradiation time as 30 seconds, the initial spot diameter as 4 mm, and the auxiliary gas pressure as 0.02 MPa.

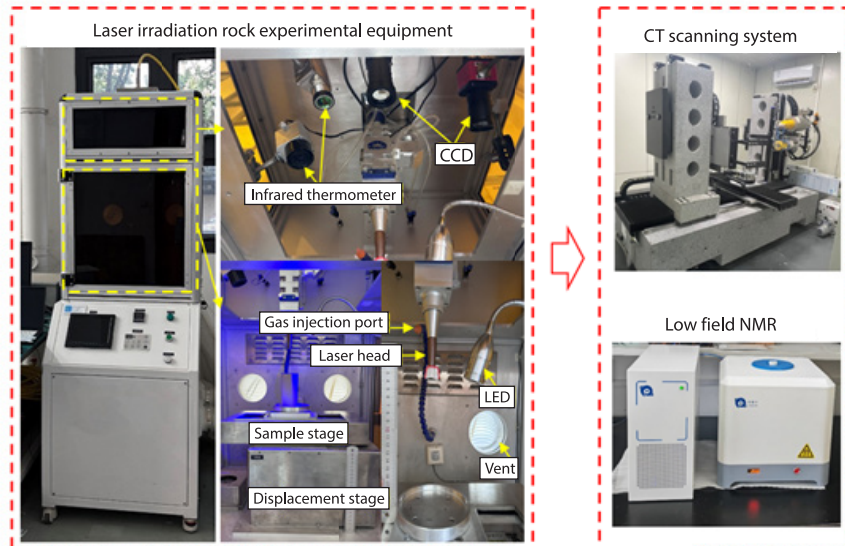


Figure 1. Experimental equipment and experimental procedure

Selected rocks in the thermally affected area after laser irradiation were prepared as $10\text{ mm} \times 10\text{ mm} \times 22\text{ mm}$ samples for low field NMR testing. These samples were vacuum-saturated with water to determine the T_2 spectrum of basalt. The test parameters are using the CPMG sequence, the test frequency is 7 MHz, the sampling bandwidth is 200 kHz, the 90° pulse width is $14.2\ \mu\text{s}$, the 180° pulse width is $26\ \mu\text{s}$, the waiting time is 1000 ms, the echo interval is 0.15 ms, the number of echoes is 2000, and the number of scans is 1024.

Results

Macroscopic damage patterns and temperature distribution

A PIX Connect-MA-E2020-05-A infrared thermometer with a range of $0\text{-}925\text{ }^\circ\text{C}$ was used to capture the temperature distribution on the rock surface and plot the temperature distribution curve. The temperature distribution over time when the 1000 W laser irradiated on the rock surface is shown in fig. 2. After laser irradiation, the rock absorbs energy and rapidly increases in temperature, following a Gaussian distribution pattern. Due to the low thermal conductivity of the rock, heat transfer is slow, resulting in the highest temperatures at the center

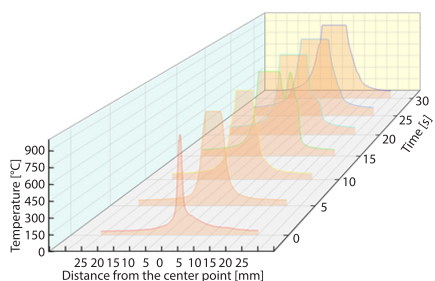


Figure 2. Temperature distribution

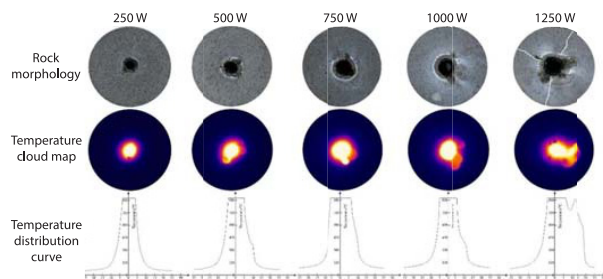


Figure 3. Rock surface morphology and temperature distribution

point which decrease rapidly towards the surrounding areas. However, as laser irradiation time increases, the high temperature region gradually enlarges. The topographic characteristics of the basalt surface after laser irradiation at different power levels and the temperature distribution on the rock surface after irradiation for the same time are shown in fig. 3. Under laser irradiation, the temperature of the rock surface increases rapidly, causing localized melting which is expelled with auxiliary gas, forming molten holes. With the increase of laser power, the range of high temperature area gradually expanded, exerting thermal stress that reaches the tensile strength of the rock, leading to the formation of tensile cracks.

Molten hole structure and 3-D reconstruction

Industrial CT was used for scanning the laser-irradiated rock and for post-processing analysis. The longitudinal section and pore formation profile of the laser-irradiated basalt are shown in figs. 4 and 5. Under laser irradiation, the basalt melted and evaporated, and the liquid melt was expelled by auxiliary gas, forming concave melt pools and small pits in the irradiated area. The laser beam directly acted on the bottoms of these pits, causing further melting and vaporization of the basalt, thereby deepening the molten holes. The depth of the pore formation and the diameter of the pore formation were quantitatively measured from the CT scan results, as shown in fig. 6. With the increase of laser power, the depth of the molten hole gradually increased, and the surface diameter of the molten hole also gradually increased. When the laser power reaches 1000 W, the surface diameter and depth of the molten hole gradually stabilize. Extracting the molten holes and reconstructing them in three dimensions, the 3-D structure of the molten holes can be obtained as shown in fig. 7. The boundary of the molten hole is rough and not completely conical, and the sidewall of the molten hole can be divided into two zones, the entrance expands outward into a drum shape, which is the expansion zone, and the lower part becomes a sharp cone, which is the V -shaped zone. This is due to the fact that the flow of molten material after rock melting is very small, although the auxiliary gas is discharged to the surrounding area, there is still a large amount of molten material accumulating in the orifice, forming a molten pool and further melting the surrounding rock.

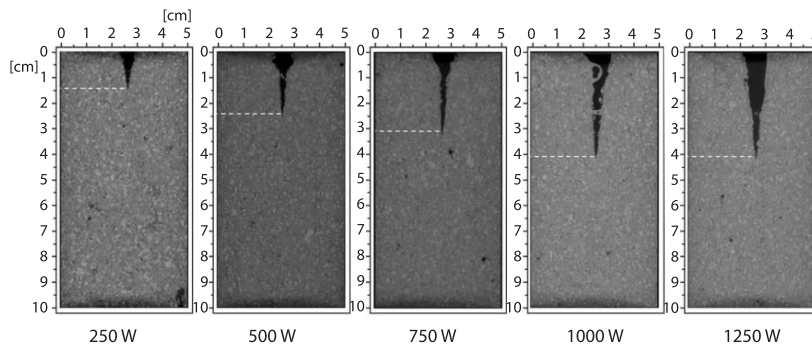


Figure 4. Profile of molten holes

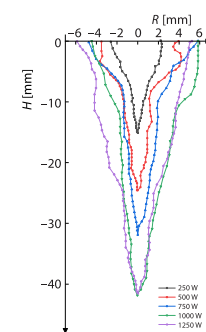


Figure 5. The outlines of molten holes

Laser power directly determines the amount of energy available to the rock. The higher the laser power, the more energy the surface of the rock material obtains per unit time. This results in faster heating rates and more significant thermal effects. The area of thermal influence is also larger, thus directly affecting the rock surface morphology and pore formation. With the increase of laser power, the accumulation of laser energy and the secondary effect of the molten

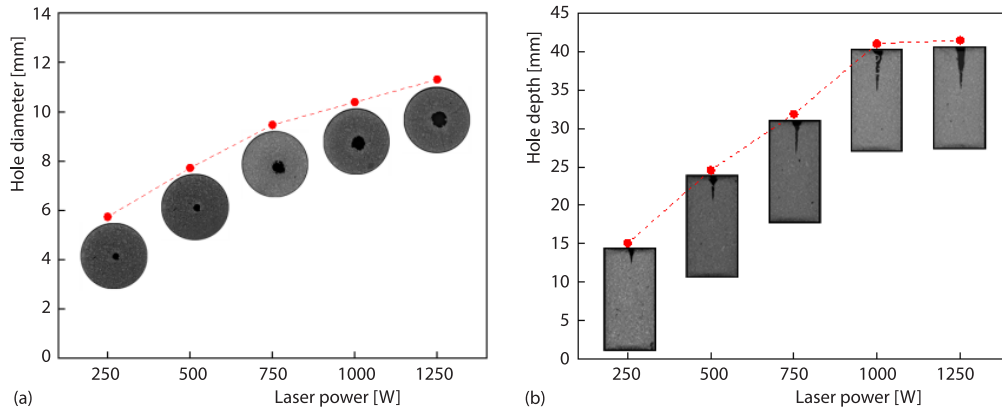


Figure 6. Variation characteristics of hole diameter and hole depth with laser power

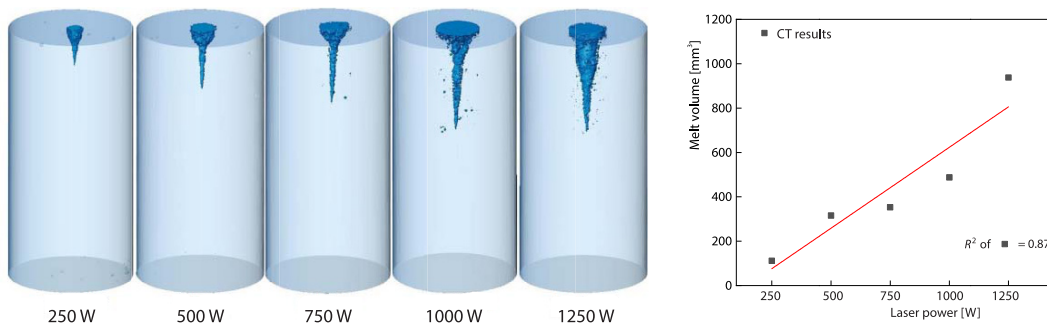


Figure 7. The 3-D pore formation characteristics of basalt after laser irradiation

Figure 8. Variation of molten hole volume with laser power

material gradually reached a balance, the depth of the molten hole no longer increases. The calculation of the molten pore volume is shown in fig. 8. The molten volume increases gradually with the increase of laser power, basically obeying a linear distribution. The 1250 W laser irradiation for 30 seconds can melt basalt with a volume of 937.7 mm³.

Quantitative characterization of basalt pore structure based on NMR technique

Low field NMR tests were conducted on the original rock samples and the rocks in the thermal affected area after laser irradiation, and the distribution curves of NMR T₂ spectra and the volume share of pore size distribution of the rocks after irradiation with different powers were obtained, as shown in figs. 9 and 10, respectively. The peaks of small pores in basalt are located around 1 ms, and the peaks of large pores are located around 25 ms, corresponding to pore diameters of 0.09 μm and 2.3 μm, and pore diameters of 0.025-0.5 μm account for 71.6% of the volume. After the low power (250 W) laser irradiation, the small pore content in the thermal affected area of basalt increased significantly, and as the laser power continued to increase, the peak value of the small pores in basalt showed a decreasing trend, and the peak value of the large pores showed an increasing trend.

Under laser irradiation, the rock absorbs laser energy. The thermal influence of the laser causes water stored in the rock's pores to evaporate, certain water-containing minerals to decompose, and thermal damage leads to phase changes and unco-ordinated expansion and

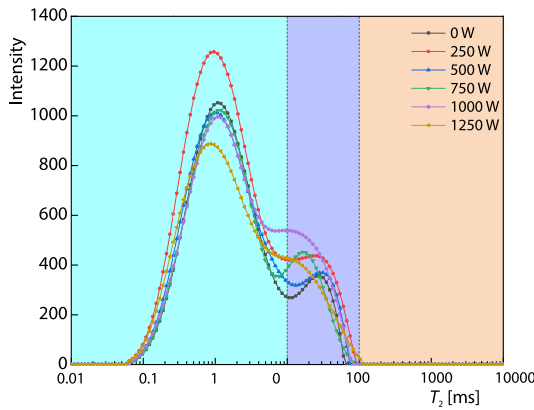


Figure 9. The NMR T_2 distribution

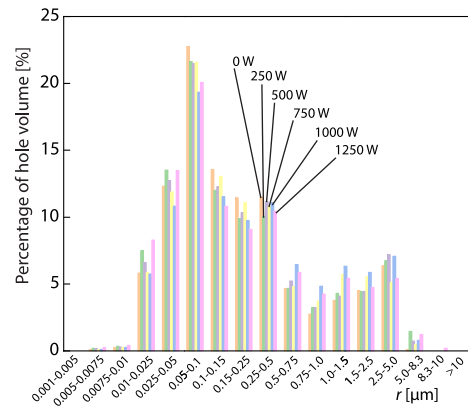


Figure 10. Histogram of small hole distribution

deformation of mineral particles, resulting in the formation of numerous tiny pores. As laser power gradually increases, thermal damage to the rock intensifies, and the destruction of the pore structure becomes more severe. Cracks may even appear when the power reaches 1250 W. Therefore, laser irradiation enlarges the radius of the pore structure inside the rock, gradually increasing the size of large pores.

Conclusion

The experimental results reported that the laser power significantly affects the laser drilling efficiency. As the laser power increases, the range of thermal influence on the rock increases, achieving a perforation depth of 41.51 mm. After laser irradiation, the sidewall of the rock molten hole can be divided into two parts: drum-shaped zones at the entrance and V-shaped zones in the middle and lower parts. This division correlates significantly with melt accumulation, and timely discharge of melt can effectively enhance laser rock-breaking efficiency. Expansion and microcracks appeared in the rock after laser irradiation. The NMR results indicate that basalt pore sizes are primarily distributed between 0.025-0.5 μm , comprising approximately 71.6% of the total. Small pores in the rock increased significantly following low power laser irradiation, and as laser power increased, these small pores gradually expanded into larger ones.

Acknowledgment

This work was financially supported by the National Natural Science Foundation of China (52225403) and the National Key Research and Development Program of China (2023YFB2390200, 2023YFF0615400).

References

- [1] Xie, H. P., et al., Mechanical Behavior of Brittle-Ductile Transition in Rocks at Different Depths (in Chinese), *Journal of the China Coal Society*, 46 (2021), 3, pp. 701-715
- [2] Li, F., et al., Formation Mechanism of Core Discing During Drilling under Deep In-situ Stress Environment: Numerical Simulation and Laboratory Testing, *Journal of Central South University*, 30 (2023), 10, pp. 3303-3321
- [3] Wang, Y., et al., Experimental Study of Thermal Fracturing of Hot Dry Rock Irradiated by Moving Laser Beam: Temperature, Efficiency and Porosity, *Renewable Energy*, 160 (2020), 2, pp. 803-816
- [4] Li, G., et al., Mechanisms and Tests for Hydraulic Pulsed Cavitating Jet Assisted Drilling, *Petroleum Exploration and Development*, 35 (2008), 2, pp. 239-243

- [5] Yin, T. B., *et al.*, Effect of High-Voltage Electric Pulse Stimulation on Heated-Granite: An Experimental Investigation, *Journal of Central South University*, 299 (2024), 2, 109935
- [6] Deng, R., *et al.*, Simulation and Experimental Research of Laser Scanning Breaking Granite, *Optics Communications*, 502 (2022), 2, 127403
- [7] Yi, X. Z., *et al.*, Temperature Fields Characteristics on Removal Rock by High-Energy Lasers, *Advanced Materials Research*, 328-330 (2011), 3, pp. 104-107
- [8] Yang, X. F., *et al.*, Investigation on the Rock Temperature in Fiber Laser Perforating, *Optik*, 219 (2020), 2, 165104
- [9] Jamali, S., *et al.*, Application of High Powered Laser Technology to Alter Hard Rock Properties Towards Lower Strength Materials for More Efficient Drilling, Mining, and Geothermal Energy Production, *Geomechanics for Energy and the Environment*, 20 (2019), 2, 100112
- [10] Guo, C. G., *et al.*, Study on the Law and Mechanics of Thermal Cracking of Rock by Laser (in Chinese), *Journal of China Coal Society*, 47 (2022), 4, pp. 1734-1742
- [11] Chen, K., *et al.*, Research on the Temperature and Stress Fields of Elliptical Laser Irradiated Sandstone, and Drilling with the Elliptical Laser-Assisted Mechanical Bit, *Journal of Petroleum Science and Engineering*, 211 (2022), 4, 110147
- [12] Pan, H. Z., *et al.*, The Influence of Laser Irradiation Parameters on Thermal Breaking Characteristics of Shale, *Journal of Petroleum Science and Engineering*, 213 (2022), 1, 110397
- [13] Zhou, X. M., *et al.*, Experimental Study on Characteristic and Mechanism of Simulated Lunar Rock Destruction under High Energy Laser Irradiation, *Thermal Science*, 27 (2023), 1B, pp. 455-463